10

EXPERIMENTAL DETERMINATION OF MECHANICAL RESPONSE OF SOLID ROCKET PROPELLANT UNDER HIGH STRAIN RATE AND LOW TEMPERATURE

by

Richard S. Culver

and

John S. Rinehart

Mining Research Laboratory
Colorado School of Mines

15 July 1964

FINAL
~~TECHNICAL~~ REPORT NO. MRL-ONR-3

Submitted to the Office of Naval Research for
work performed under Grant No. Nonr-3774-(00) (FMB)

ABSTRACT

Described in this report are the results of an experimental investigation of the mechanical properties of two simulated solid rocket propellants. The "green" propellant is salt-filled polyurethane; the "gray" propellant is Adiprene L-100, filled with aluminum powder, aluminum sulphate, and castor oil.

In low temperature tests there was found the expected inverse relation between temperature and U.T.S. For the green propellant, the U.T.S. varied from 170 psi at room temperature to about 6,000 psi at -200°C, while corresponding values for the gray were 250 psi and 11,000 psi, respectively.

In static torsion tests, the gray propellant exhibited a marked notch sensitivity and a tensile fracture mode, while the green had no notch sensitivity and a shear fracture mode.

The impulsive fracture strength of the green propellant was found to be about 16,000 psi, in confirmation of tests run by previous investigators, and the shock attenuation at this stress level is about 5,000 psi/in. An approximate value of 24,000 psi for the impulsive fracture strength of the gray was obtained by indirect means, along with a shock attenuation of 1,500 psi/in. On the basis of these fracture strengths,

calculated points on the Hugoniots of the two propellants were obtained.

The dynamic Poisson's ratio for the green propellant was found to be greater than 0.5, while for the gray, it was less than 0.5. Both propellants have static values of ν in the range of 0.5.

A deformation wave velocity was discovered which travels at a velocity of 400 fps in the gray propellant and 1,000 fps in the green.

I. INTRODUCTION

As discussed in the last progress report, the current research has been carried out in three phases: cold temperature tensile tests, impulsive spallation tests, and dynamic compression tests to determine the dynamic Poisson's ratio for solid rocket propellant.

1.0 Materials Tested

Two propellants were tested in varying degrees in each setup. These will be referred to as the "green" and "gray" propellants on the basis of their respective physical appearance. Both propellants are inert and resemble actual propellant only in their mechanical properties.

The green propellant, designated DP-16, is polyurethane based with a salt filler, and it was supplied by Aerojet General Corporation. Its composition by percent is:

Polyurethane	15
Potassium Chloride	85

The gray propellant, supplied by the Southwest Research Institute, has the following composition by percent:

Adiprene L-100	16
Castor Oil	6
Aluminum Powder	22
Aluminum Sulphate	56

II. LOW TEMPERATURE TENSILE TESTS

2.0 Introduction

In an attempt to relate the low temperature mechanical properties of solid rocket propellant to its dynamic mechanical properties, a series of low temperature tensile tests were run on the two propellants investigated. These tests were designed to measure the stress-strain relation, to failure, at five temperatures: ambient, 0°C, -10°C, -80°C, and -200°C. Due to peculiarities in the mode of fracture in these tests, a quick series of torsion tests was also run to investigate the effect of shear deformation.

2.1 Apparatus and Test Procedure

2.1.1 Test Machine and Specimen

The tensile tests were run on a Tinius Olsen Universal Testing Machine. It was necessary to construct special grips and load cells in order to test the propellant properly.

The initial grips were designed on the principle of a collet and were used to hold an 8 in. x 1 in. diameter specimen, with a neck diameter of 0.6 in. (Fig. 2.1). This specimen configuration was a modification of the standard specimen described in the Federal Test Method Standard for the tensile testing of plastics. This arrangement had two drawbacks: the specimen slipped out of the grips as its cross sectional area decreased, and it was difficult to

turn the propellant on a lathe.

For these reasons a new set of grips was made to fit a JANAF type specimen (Fig. 2.2). These specimens could be made quite easily on a milling machine, and when tested, they slipped freely in the grips until snuggly seated. As with the previous grips, attachment to the testing machine was made through a ball and socket coupling to assure axiality of alignment. This should have allowed a uniform tensile stress across the test section. It was found that due to inherent inaccuracies in the machining of the specimens, the circular shoulders against which the grips pulled were not always evenly spaced. This out-of-alignment, which was seldom more than 1/64 in., was difficult to see with the eye, and could only be corrected in the more severe cases. At temperatures high enough for the specimen to deform until seated, this out-of-alignment caused no serious problem, but at very low temperatures, it appears to have affected the results. This will be discussed further in section 2.2.1.

The cold trap used to hold the coolant was, for the ice and dry ice, a Plexiglas, double-walled tank. The Plexiglas was used in order to allow visual observation of the deformation, but it was found that condensation and the murkiness of the coolant precluded this. Because of its superior insulating properties, a polystyrene foam tank was constructed for use in the liquid nitrogen tests.

There was some question as to whether the coolant, which was in direct contact with the specimen, might attack the specimen and affect its mechanical properties. Therefore, in the early tests in which coolant was used, the specimens were coated with "Silastic", a low-modulus, synthetic rubber, which would not adhere to the specimen. The Silastic served the further purpose of providing a thermal barrier which lessened the thermal shock when the specimens were first submersed in the coolant. It was found that for the dry ice and liquid nitrogen tests, there was no effect on the tensile strength when the Silastic was left off, so its use was discontinued.

2.1.2 Instrumentation

Two load cells, using wire strain gage sensing units, were made — one covering the range from 0 to 500 lbs. and the other covering the range from 500 to 1500 lbs. These were placed in the load train as indicated in Fig. 2.2.

Because the specimens slipped in the loading grips, it was necessary to measure the deflection directly on the specimen, rather than the relative motion of the grips. It was found that this could most easily be done by measuring the change in lateral dimensions of the neck. This was done with a split steel ring which rested on either side of the neck. Strain gages recorded its change in radius, thereby indicating the change in specimen cross section. This

technique conveniently measures to an accuracy of 0.001 in. Because an accurate value of Poisson's ratio is not available, an approximate calculation of the longitudinal strain was made assuming $\nu = 0.5$.

While it was originally intended that the strain be determined in all tests the total strain to fracture was so small in the two lowest temperature tests, that its determination did not seem to warrant the complications involved. In the final analysis of the data, the strain was only considered in those cases where it was large enough to affect the stress.

All records of the tests were made on the basis of load, and in some cases deflection, as a function of time. Usually readings were made every 15 seconds. It will be convenient, therefore, to record the results of the higher temperature tests in terms of an average strain rate, and the two lowest temperature tests in terms of an average load rate.

2.1.3 Torsion Test Apparatus and Procedure

As will be discussed in the results, the mode of fracture of the gray propellant appeared to be quite different from that of the green, and so it seemed worthwhile to compare their fracture strengths under pure shear strain. It was decided that a torsion test on a hollow tubular specimen would be the simplest means of obtaining a state of pure shear in

the specimen. The minimum cross section used in the tests was 1.25 in. ID and 1.85 in. OD.

An improvised torsion testing machine was made out of a lathe by gripping one end of the specimen in a four-jaw chuck and supporting the other end on a center in the tail stock (Fig. 2.3). A torque arm was attached to the tail stock end of the specimen and a bucket was hung on the end of the torque arm so that shot could be poured into it.

As the first specimen failed by buckling, the successive specimens were made as short as possible, and a steel rod was imbedded in the rotating end of the specimen and passed through a journal bearing in the fixed end to supply additional lateral stiffness.

The specimen was loaded by slowly pouring shot in the bucket until the first sign of gross relaxation of the specimen. The only precise measurement made was the fracture torque. Rough measurements of the fracture shear strain indicated that it was approximately one, i.e. 45°.

2.2 Test Interpretation and Results

2.2.1 Tension Tests

Several tests were run at each temperature on both types of propellant. Most of the results given in Table 1 (and Fig. 2.4) were obtained from the JANAF type specimen, although a few confirmatory tests were run using the

cylindrical specimens, both at room temperature and at liquid nitrogen temperature. As no apparent difference was obtained, these tests are not identified in the table.

As mentioned in section 2.1.2, the recorded maximum strain, and strain and load rates, are only approximate values and are included primarily for comparison. The UTS (fracture strength) values given for the tests at ambient, 0°C, and -10°C, are calculated on the basis of the load divided by the cross sectional area at fracture.

There appear to be three main reasons for the variation in UTS obtained and recorded in Table I: variation in strain rate, nonaxiality of loading, and rate of cooling. While no extensive attempt was made to separate these effects, the general effect of strain rate may be seen by referring to the values in Table I. The effect of the other two was minimized insofar as was possible. It should be added that a certain amount of variation resulting from the inhomogeniety of the material (particularly in the green propellant) would be expected.

Thermal shock was found to affect the UTS of the specimens primarily in the liquid nitrogen tests. The green propellant was found to have a significantly higher UTS when cooled in stages: the specimen was placed ir a copper cannister which was first placed in dry ice, then in liquid nitrogen, and finally in direct contact with the liquid

nitrogen. In the dry ice tests, the specimens were first cooled in powdered dry ice, and then alcohol was mixed with the dry ice to improve heat transfer and maintain a uniform bath temperature around the specimen during the test.

As mentioned in the discussion of apparatus, inaccuracies in machining the specimen are presumed to have affected the stress distribution across the neck in some of the JANAF type specimens. In the room temperature tests, where the average strain in the neck was in the order of 0.2, a variation of a few hundredths in the shape of the grips and specimen would not affect the results, but at dry ice and liquid nitrogen temperatures, the total strain was only a few thousandths, so the smallest misalignment could subject the specimen to a considerable bending moment. This is assumed to account for most of the large variation in UTS obtained at the lowest temperatures, and for this reason, the highest values will be considered the most valid.

In order to minimize the alignment problem, a pivot was built directly into the top grip in order to facilitate alignment of the specimen.

It also appeared that it might be possible to seat the specimens by prestressing them at a low value before testing, thus decreasing the nonuniformity across the cross section during testing. A specimen of each material was tested at room temperature by first preloading it up to about 50 psi

and leaving this load on it for about 20 minutes. The green specimen had relaxed about 15 psi and the gray about 25 psi. The specimen was then loaded on to fracture in each case. The gray showed no appreciable effect of the preload, but the green broke at a UTS of 110 psi or about 2/3 the UTS in the other tests. This reduction in strength is assumed to be related to the creep properties of the material.

The actual fracture which occurred was "ductile" in the room temperature and ice water tests, i.e. the fracture started from a crack causing the specimen to neck down and slowly tear apart. The fracture was always a tensile fracture, normal to the tensile axis.

While it was found that in general the gray propellant was about 50% stronger than the green, any small stress concentration, particularly a notch normal to the tensile axis, would severely decrease its strength. The gray specimens also had a tendency to break well up in the jaw at the point of maximum compressive load. The fracture would start out normal to the jaw and run in a circular arc over to a corresponding point on the other jaw.

At the lower temperatures the fracture was "brittle", the specimen breaking with a sharp crack. As in the room temperature tests, some of the gray specimens broke well up in the jaw of the grip, the crack apparently propagating from the point of contact with the jaw.

2.2.2 Torsion Tests

Because of the peculiar notch sensitivity exhibited by the gray propellant, it appeared worthwhile to determine the shear fracture strength and specifically the effect of notches on the fracture strength.

The results of the torsion test showed a distinct difference in the basic mode of fracture between the green and gray propellants (See Table II). While in both cases the shear strength was comparable to the tensile strength, the green propellant consistently failed in a shear type fracture, in the plane of the maximum torque. The gray propellant, conversely, failed in tension on a helical plane.

The other result of interest was that the gray propellant was extremely sensitive (about 50 percent reduction in strength) to small surface cuts which were made on the surface of the neck (about 1/32 in. deep and 1/2 in. long). These cuts were placed at 0°, 45°, and 90° with the axis of the specimen in order to compare the influence of the direction of the cut. Conversely, the green propellant showed essentially no sensitivity to the notches at all*.

*All calculations of the maximum shear stress were based on the equation

$$\tau = \frac{Tc}{J}$$

where τ is the shear stress, T is the torque, J is the Polar Moment of Inertia, and c is the distance from the central axis to the outside surface of the neck or to the bottom of the notch or cut.

III. IMPULSIVE LOADING TESTS

3.1 Introduction and Background

The impulsive loading tests were run on the air gun apparatus described previously in the report by Charest, et al[1]. Basically the purpose of the current series of tests was to confirm the results previously published and to extend them to include th spallation strength of the gray propellant.

In order to explain the purpose of the present test program, it seems in order to review the theoretical basis of the experiment and some of the experimental problems encountered by the previous investigators.

The spalling technique as a means of determining the impulsive fracture strength of a material is based on the hydrodynamic theory of wave propagation. According to this theory, a compressive wave traveling normal to a free surface will be reflected at the free surface as a tensile wave of identical shape. If the maximum amplitude of the tensile wave is equal to the fracture strength of the material through which it is traveling, the material will fracture when the head of the tensile wave has passed the tail of the compressive wave. Before the tensile wave reaches the fracture plane the net stress at each point in the material is the algebraic sum of the tensile and compressive stress components at that point. Thus the position of the spall, or fracture, and the amplitude of the incident wave required to produce

it will depend on the shape of the wave. The impact of a flat plate on another flat plate theoretically produces an ideal square compressive stress pulse whose length in time is:

$$t = \frac{2\lambda}{c_s} \tag{3.1}$$

where t is the time, c_s is the shock wave velocity in impactor, λ is the thickness of impactor. The amplitude of the stress pulse is:

$$\sigma = \frac{\rho_{20}}{\delta_2}\left(\frac{V_o}{1+\sqrt{\frac{\rho_{20}\ \delta_1}{\rho_{10}\ \delta_2}}}\right)^2 \tag{3.2}$$

where σ is the stress, ρ_o is the unstressed density, δ is the change in density $\frac{\rho}{\rho_o} - 1$, and V_o is the impact velocity.

Thus, in order to determine the stress, the Hugoniot (the dynamic equation of state) must be known for the two impacting materials. If the target and impacting materials. If the target and impacting plate are made of the same material, Eq. 3.2 reduces to

$$\sigma = \frac{\rho_{20}}{\delta_2}\ \frac{V_o^2}{4} = \rho_{20}\ c_s \frac{V_o}{2} \tag{3.3}$$

so the stress may be determined through a knowledge of the impact velocity and the Hugoniot of the material. As it is usually possible to measure the shock velocity, the use of the same material for impactor and target is a convenient method of determining the Hugoniot for a material.

Thus far, no consideration has been given to the attenuation of the stress wave. For most solid materials tested in the manner described above, the attenuation of the stress wave as it travels through the target plate is small enough so that it can be ignored. Attenuation begins to become serious when the stress level is high enough to cause a noticeable change in the density*. For most materials with a large bulk modulus, i.e. small value of δ for a given stress, the fracture strength will normally occur at a level corresponding to a comparatively small change in density. The propellant materials being tested have a very low bulk modulus and thus show a considerable attenuation of the incident stress pulse, as well as variation in the shock velocity.

The attenuation of the stress pulse changes not only its amplitude but also its shape. One of the principles applied in the hydrodynamic theory is the conservation of momentum, which states that in the collision of two freely moving bodies the area under the pressure-time curve is constant. Thus, if a square wave is introduced into a propellant target, it will become longer in time as the pressure amplitude decreases. This infers that different portions of the wave must travel at different velocities,

---

*The change in density δ and shock velocity are related by the Equation $\delta = -\frac{V_o}{2c_s}$.. The bulk modulus of a material is defined as the ratio of impact stress to density change, σ/δ, and is obtained from the slope of the Hugoniot.

which is reasonable since the lower the stress amplitude, the slower the stress wave travels. It would be expected therefore, that the stress wave reflected at the free surface would be roughly wedge-shaped, instead of square.

It can be seen that with the decay of the stress amplitude and shock wave velocity occurring at various rates throughout the stress pulse, the determination of the conditions causing the spall to form will be very difficult and would require a knowledge of the pressure-time profile at the free surface, the Hugoniot, and the rate of stress attenuation. The test series undertaken was designed to provide this background information for use in analyzing the data obtained in the spallation tests.

3.2 Planarity Tests

In all the tests run with the air gun, the planeness of impact between the two colliding surfaces is extremely important. All simplifying assumptions on the noninterference of edge effects, recording the rise time of the pressure pulse, etc., are based on a plane impact. As an indication of the problem, for an impact velocity of 300 fps, a tilt of 0.001 in. across the impact surface would cause a tilt of over 0.02 in. in the stress front traveling through propellant, and about 0.06 in. in steel.

To assure alignment of the impacting surface, a ground plate was fabricated with four insulated pin-contacts mounted

flush with the plate surface. These pins were placed in a triangular array with one pin at the center, thus allowing measurement of both the tilt and the flatness of the impactor with respect to the plate. The pin contacts were connected, through an electrical circuit, to two high speed oscilloscopes where the time of arrival of the projectile to each pin was recorded.

Repeated tests with this arrangement indicated a random misalignment of over 0.001 in. tilt. This was traced to a flared end on the gun barrel which allowed about 0.003 in. clearance around the projectile in the last few inches before impact. When it became apparent that O-ring bushings, runners, and other types of spacers would not eliminate this problem, a new gun barrel made to closer tolerances was ordered. After suitable alteration of the specimen holding devices, the tilt was kept consistently below 0.0005 in. This precision was sufficient to assure a reasonable percentage of acceptable tests.

3.3 Quartz Transducer Technique

In order to determine the pressure profile and peak pressure amplitude, which is needed in both the determination of the Hugoniot and pressure attenuation, the quartz transducer technique described by Charest, et al,[1] is the most direct procedure available. Considerable effort was expended in an attempt to get meaningful traces from the setup described in

the previous report, but no satisfactory arrangement was obtained. The limited time available prevented consultation with other investigators who have successfuly used this technique.

Had this technique been perfected, the procedure was to have been as follows:

1. In order to eliminate the pressure decay from consideration, an aluminum target would be impacted with a propellant projectile. Since the pressure decay in the aluminum is small and can be accounted for, an accurate determination of the pressure-impact velocity relation could be obtained. From this, by knowing the Hugoniot of the aluminum, the Hugoniot of the propellant could be determined.
2. By impacting the propellant with an aluminum impactor, the pressure decay could be determined, since the pressure at the impact surface is known and the pressure on the free surface could be measured.
3. While the quartz transducer will only record the first portion of the pulse (approximately 1 sec) the length of the pulse can be estimated from the thickness of the spall, so that it should be possible to estimate the shape of the entire wave profile.

3.4 Spallation Tests

3.4.1 Test Program

Since, as was discussed in the previous section, it was not possible to measure the spalling stress directly, it was necessary to devise indirect means of estimating the spalling stress, or more exactly, the impact stress and the attenuation of the stress pulse. Basically, these indirect means consisted of determining the critical spalling velocity (the minimum impact velocity which would cause a spall) and undertaking various other auxiliary tests which gave an indication as to the shape of the Hugoniot for the two propellants. The spalling velocity was determined for various thicknesses of propellant targets, and four different impact materials. The auxiliary tests which were run consisted of a static determination of the equation of state of the propellants and measurement of the acoustic wave velocity and shock velocity by several different means. The auxiliary tests will be discussed first.

The static equation of state for the two propellants was measured by compressing cylindrical specimens in a close-fitting steel chamber. To avoid inaccuracies due to voids in the chamber, the initial portion of the curve up to about 2 percent volume change was disregarded. The curves obtained are shown in Fig. 3.1, along with the Hugoniot of Plexiglas, aluminum, and various calculated points on the Hugoniots of the two

propellants which will be discussed later. As was suspected, the gray propellant exhibited a significantly lower bulk modulus than the green.

The acoustic wave velocity was measured by an apparatus consisting of two piezoelectric crystals, one serving as a transmitter and the other as a receiver, which were placed on opposite sides of a block of propellant. It was found that a small increase in the clamping pressure used to hold the crystals against the propellant block made a substantial difference in the measured wave transit time. A 5 percent increase in the calculated velocity was obtained with moderate pressure. The minimum values which could be consistently obtained were:

for the green, c_a = 5600 fps

for the gray, c_a = 5060 fps

The shock velocity, i.e. the velocity of a discontinuous wave front of large amplitude, will obviously vary with stress amplitude and degree of compression of the transmitting medium as has been discussed, so it is only possible to obtain a representative value for stress amplitudes in the range of interest. In both the previous and current investigations, attempts to measure the average velocity of the stress pulse through the propellant target yielded very inconsistent results and was discarded as a test procedure. Charest, et al[1], reported an experimentally determined value of c_s = 6500 fps for the

green propellant which was obtained by measuring the transit time of the shock wave from a blasting cap in a block of propellant. Unfortunately, since there is no way of knowing the amplitude of the stress pulse, it is at best an approximate value.

Another determination of the shock velocity of the green propellant was obtained by placing a sheet explosive charge on one side of a rectangular block of propellant. When detonated on one end, the explosive sends a shock wave into the propellant which makes an angle with the explosive surface which is determined by the ratio of detonation velocity in the explosive and the shock velocity in the propellant. A corner fracture of the same angle is obtained in the corner of the propellant diagonally opposite from the point of initiation. This procedure was followed for blocks of various thicknesses and the results indicated a maximum value for 1/2 in. thick block of over 20,000 fps. The shock velocity decreased to a minimum value of 6,500 fps for a block 1 1/2 in. thick. Since both investigations found a limiting value of 6,500 fps, it is thought likely that this value corresponds to a stress level of approximately 10,000 psi at which the previous investigators found attenuation to have become negligible. It is of interest that the detonation pressure of the explosive, 3 million psi, has decayed, without divergence, to a value of about 10,000 psi in a distance of 1 1/2 in.

Attempts to measure the shock velocity in the gray propellant with the blasting cap technique gave values varying from 6,000 to 8,000 fps. It was decided that a more representative and directly comparable value could be obtained by calculating a shock velocity from the value of 6,500 fps used for the green propellant. The calculated value is 6,600 fps. Details of its calculation are given in the following section.

3.3.2 Test Results and Interpretation

The critical spalling velocities for various impactors and target thicknesses are given in Table III. The impact stresses listed are determined from Eqs. 3.2 and 3.3. It will be noted that there is considerable scatter in the velocities and stresses. It was not uncommon to obtain no spall at impact velocities significantly above those quoted. For this reason, the exact spalling velocity is in question in most cases. It is likely that the rapid attenuation of the initial high amplitude stress pulse decreases the effect of variations in impact velocity, making small variations in impact geometry and irregularities in the propellant structure abnormally important.

The impact stress for the green propellant was determined by use of Eq. 3.3, c_s = 6,500 fps, and V_o = 280 fps, to be 20,200 psi. The corresponding value of σ is found from the relation, $\sigma = V_o/2C_s$, to be 0.021. As an independent

check on this value, it will be noted that the spalling velocity for Plexiglas is approximately 280 fps, which is the same value obtained with a propellant impactor. This apparently indicates that the impact stress is also equal to that of a propellant impactor. Using this condition, Eq. 3.2 reduces to,

$$\frac{\rho_0 \text{ propellant}}{\rho_0 \text{ plexiglas}} = \frac{\delta \text{ propellant}}{\delta \text{ plexiglas}} \qquad (3.4)$$

From this relation, it is possible to make use of the known Hugoniot of Plexiglas in order to calculate a point on the propellant Hugoniot. At a stress of 20,000 psi, Eq. 3.4 gives a value of $\delta = 0.026$.

It is now necessary to extend this procedure in order to obtain a point on the Hugoniot of the gray propellant. Two possible approaches exist. The first is to move the static equation of state by an amount equal to the ratio of dynamic to static equation of state for the green propellant. The resulting point (No. 3) is plotted in Fig. 3.1. Using Eq. 3.3, $V_0 = 505$ fps, and $\delta = 0.055$, a value of the impact stress of 26,000 psi is obtained. In the second procedure, a reasonably realistic estimate of the shock velocity is determined from the ratio between shock velocity and acoustic velocity for the green propellant. This estimated shock velocity is obtained from the relation:

$$\left(\frac{c_s - c_a}{c_a}\right)_{gray} = \frac{\delta_{gray}}{\delta_{green}} \left(\frac{c_s - c_a}{c_a}\right)_{green} \qquad (3.5)$$

A value of 6,600 fps is obtained in this way. Using this value, the impact stress is 38,500 psi, and = 0.039. This point falls on the calculated Hugoniot for the green propellant (See Fig. 3.1, point No. 4). For the acoustic wave velocity of the gray propellant, an impact stress of 29,000 psi is obtained (point No. 5, Fig. 3.1) which suggests that the value of 26,000 psi obtained by the first procedure is probably low.

A good estimate of the attenuation of the stress pulse is difficult because of its strong dependence on the value of the stress. It was decided that a logarithmic relation would best represent the stress as a function of the distance from the spalling plane. It is interesting that, if the results of the previous investigators when using this experimental technique are plotted on a graph of log stress versus distance from the impact plane, a fracture strength value of 16,500 psi is obtained which is significantly closer to the fracture strength obtained by the two other techniques, than their quoted value of 14,300 psi based on a linear attenuation of stress (See Fig. 3.2).

In order to determine the attenuation of the gray propellant, the best data available is that using a Plexiglas impactor. The values of impact stress determined from Eq. 3.3, using the minimum value of for the gray propellant (that corresponding to an impact stress of 38,500 psi) are given in Table III. By drawing a representative line through these four points, Fig. 3.2,

an indication of the degree of attenuation may be obtained. If lines of the same slope as this one are drawn through the maximum and minimum values of impact stress, it is found that the spalling stress lies in the range of 21,000 to 27,000 psi.

The average impulsive fracture strength for the green propellant is 16,000 psi. It was found in the cold temperature tensile tests that the gray propellant is about 50% stronger than the green. On this basis, a nominal value of the fracture strength for the gray propellant of 24,000 psi would appear reasonable. The attenuation in this stress range is approximately 1,500 psi/inch.

IV. DETERMINATION OF POISSON'S RATIO

4.1 Introduction

An important parameter in the determination of stress distribution in a deforming body is Poisson's ratio. This ratio had tentatively been determined in preliminary investigations on the green propellant to be greater than 0.5 which is the usual value for rubber-like materials. To confirm the earlier results and extend the range of strain rates considered, an apparatus was constructed which would simultaneously record the longitudinal and lateral strain in a deforming propellant specimen.

To establish the method of defining Poisson's ratio, it is convenient first to look at the case of constant volume for which $\nu = 0.5$. Starting with the relation,

$$\text{Vol} = AL$$

differentiating,

$$d(\text{Vol}) = AdL + LdA = 0$$

Therefore

$$dL/L = -dA/A$$

which, when integrated, gives,

$$\ln L/L_o = \ln A_o/A$$

Now, $A = \pi D^2/4$, so:

$$\ln L/L_o = \ln D_o^2/D^2 = 2\ln D_o/D$$

giving

$$0.5 = \frac{\ln Do/D}{\ln L/L_o} = \nu$$

Poisson's ratio can be derived in a manner similar to that above for non-constant volume deformation giving the relation,

$$\nu = \frac{\ln D_o/D}{\ln L/L_o}$$

4.2 Apparatus and Test Procedure

The specimen used in this test setup was a cylindrical slug of propellant, 1 in x 0.8 in dia. It sat on a brass pedestal upon which strain gages were mounted in order to record the load. A 6 foot, vertical air gun was placed above the specimen at velocities varying from 20 to 200 fps. The weight of the projectile was adjusted to obtain an approximately constant maximum deformation of about 3/8 in. For a strain greater than about 40 per cent, the bulging became serious and the specimen tended to slip over the edge of the impactor. Furthermore, since the strain rate continuously varied throughout the impact, the clearest presentation of the results would be a plot of ν as a function of the progress of the impact for various impact velocities. This comparison would only be meaningful for a uniform degree of deformation.

In addition to the load measurement from the strain gages, the incremental strain is recorded on a drum camera recorder. The specimen is first painted white and then blackened with lamp black, leaving masked white horizontal and vertical lines.

A specially designed optical arrangement projects a point image of each line on the recording film, which is mounted on the rotating drum. The rotational speed of the drum establishes the time base of the record. In addition, 2.5 millisecond timing marks are superimposed on the film with a stroboscope. As deformation progresses, the point images move perpendicular to the film motion, giving a continuous record of the longitudinal and lateral strain profile throughout the impact. The strain could be determined from measurements taken from the film to an accuracy of about 5 per cent strain. Accuracy to about 1 per cent strain is possible with this technique.

4.3 Discussion of Results

Representative curves of ν versus longitudinal strain for the two propellants are given in Figs. 4-1a and 4-1b. It can be seen that the green propellant tends to have a value of greater than 0.5, while the gray is less than 0.5. The static values in both propellants are relatively constant at about 0.5.

Accurate determination of ν was hampered by both limitations in the experimental technique and the complex nature of the propellant. It can be seen that since the strain is only accurate to about 5 per cent, for low values of strain, the possible error in the determination of ν

could be as much as 100 per cent or more. On the other hand, the strain was very non-uniform for large deformations, which meant that it was necessary to measure the lateral and longitudinal strains on the same cross sectional plane for a meaningful value for ν. Since the lateral strain was always measured on the same cross section, it was necessary to make the assumption that the center portion of the specimen deformed uniformly.

Nonaxiality in loading caused further inaccuracy in the results since the longitudinal and lateral strains were measured on planes displaced 90° around the specimen. Therefore, depending upon the degree and orientation of the bending of the specimen, the calculated value of ν might be consistently high or low. This misalignment was an inherent limitation of the test apparatus which resulted from the poor interior surface on the gun barrel.

Considering these complications, it is not surprising that it has only been possible to indicate the trend of the Poisson's ratio. Undoubtedly, the apparatus and test technique could be refined in order to give an acceptable value for ν if it were deemed worthwhile. It appears possible to make a useful record for impact velocities up to 300 fps or more. However, it was found that at the higher impact velocities the attenuation of the stress wave caused the deformation of the specimen to be non-uniform, with a roughly conical

shape occurring. This was related to another observed phenomena; there was a definite limiting velocity of propagation at which a finite amount of deformation would travel along the axis of the specimen. This velocity was about 400 fps for the gray propellant, and 1,000 fps for the green. It is not known what the significance of these deformation waves is, but they might conceivably define a lower limit to the strain rate at which brittle-like behavior occurs. It would seem that this phenomena might warrant further investigation.

V. CONCLUSIONS AND SUMMARY

In all the test programs it was found that the peculiar properties of the propellant created special problems not normally encountered in these tests. Conversely, because the tests were designed to investigate untested parameters of the propellant, the standard propellant testing techniques were of limited use. It is hoped that the techniques discussed in this report will be of some use in designing future experimental programs.

In the low temperature tests, there was found the expected inverse relation between temperature and ultimate tensile strength. For the green propellant, the UTS varied from 170 psi at room temperature to about 6,000 psi at -200°C, while the corresponding values for the gray propellant were

250 psi and 11,000 psi, respectively.

It was also found that the gray propellant has a marked notch sensitivity while the green is apparently insensitive to notches. Static torsion tests run to investigate this phenomena yielded the following results:

1. small cuts on the gray propellant reduce its strength by 50 per cent;
2. the ultimate shear strength of the green propellant is approximately 150 psi, for the gray it is about 270 psi;
3. the green propellant failed in a shear fracture, while the gray failed in a tensile fracture.

The impulsive spallation tests which were run confirmed the results obtained for green propellant by the previous investigators. The impulsive fracture strength for the green propellant is about 16,000 psi, and the attenuation at this stress amplitude is about 5,000 psi/in. By indirect techniques in which the gray propellant was compared with the green, an approximate impulsive fracture strength of 24,000 psi was obtained for the gray, with an attenuation at that stress level of 1,500 psi/in. On the basis of these fracture strengths, calculated points on the Hugoniots of the two propellants were obtained.

Dynamic compression tests were run to determine the dynamic value of Poisson's ratio for the two propellants, but inherent inaccuracies in the testing technique precluded an accurate determination of ν. The trend of all the results indicated that ν for the green propellant is greater than 0.5, while for the gray propellant, it is less than 0.5. For both propellants, the static value is very nearly 0.5. It was also found that the initial wave of finite deformation traveled at a definite velocity, considerably below the acoustic wave velocity. This deformation wave velocity is approximately 400 fps for the gray propellant and 1,000 fps for the green. It is thought possibly that this velocity might be related to a critical strain rate above which the propellant behaves in a brittle manner. No proof of this suggestion is available.

BIBLIOGRAPHY

Charest, J. A., Bichot, B. H., and Rinehart, John S., A determination of the dynamic tensile strength and shock attenuation of simulated solid rocket propellant, Technical Report No. MRL-ONR-1, Office of Naval Research, August 1, 1963.

ACKNOWLEDGMENT

The authors wish to acknowledge the able assistance of Mr. Jack Kintner, Mr. Bob Anderson, Mr. Larry Frush, and Mr. George Costello in the construction of the equipment and running of most of the tests.

TABLE I. Cold Temperature Tensile Tests

Specimen Number	U.T.S.(psi)	Approximate Max. Strain	Strain Rate(/Min)
Room Temperature			
1Y*	160	0.14	0.07
2Y	185	0.14	0.07
3Y	160	0.13	0.04
4Y	167	0.13	0.04
1G**	250	0.35	0.03
2G	234	0.30	0.04
3G	270	0.25	0.06
4G	235	0.25	0.06
0°C Coolant: ice and water			
21Y	176	0.14	0.01
22Y	231	0.14	0.06
21G	344	0.2	0.02
-10°C Coolant: ice and salt			
31Y	209	0.10	0.01
32Y	178	0.10	0.02
31G	370	.12	0.03
32G	328	.12	0.05

*Y = Green Propellant

**G = Gray Propellant

TABLE I (Cont'd) Cold Temperature Tensile Tests

-80°C Coolant: dry ice and alcohol

Specimen Number	U.T.S.(psi)	Load Rate(lb./Min)
41Y	2070	500
42Y	2270	500
43Y	2130	130
44Y	2830	120
45Y	2780	1800
46Y	2830	120
47Y	2800	250
41G	4080	250
42G	4270	300
43G	4520	300

-200°C Coolant: liquid nitrogen

51Y	2,320	200
52Y	6,660	500
53Y	4,370	500
54Y	4,340	500
51G	11,680	1,200
52G	8,040	700
53G	10,980	1,000
54G	5,520	600
55G	6,000	500
56G	5,730	500
57G	7,330	900

TABLE II. Torsion Tests

Specimen Number	Ultimate Shear Strength, psi	Fracture Mode	Remarks
1YS	137	Shear	Rapid load
2YS	120	Shear	Slow load
3YS	155	Shear	Slow load
4YS	132	Shear	Slow, Oblique notches, 1/32 - 1/16 in. deep
5YS	147	Shear	Slow, Circumferential notch, 0.02 in. deep
1GS	206	Tensile	Slow, Broke in fillet at corner
2GS	270	Tensile	Slow, Helical fracture plane
3GS	154	Tensile	Circumferential notch, 0.02 in. deep
4GS	125	Tensile	Oblique notches, 1/32 - 1/16 in. deep
5GS	128	Tensile	Oblique notches, 1/32 - 1/16 in. deep

TABLE III. Minimum Spalls

GREEN PROPELLANT

Impactor	V_o* (fps)	Spall Thickness	Impact Stress (psi x 10^{-3})	Specimen Thickness (in)
1.4" Plexiglas	287	1/8"	21.0	0.490
1/8" Plexiglas	283	3/16"	20.3	0.490
1/8" Plexiglas	260	3/16"	18.0	0.490
1/4" Aluminum	254	7/32"	26.5	0.490
3/16" Aluminum	248	7/32"	25.7	0.490
1/8" Aluminum	232	7/32"	24.0	0.490
.09" Steel	221	3/32"	27.0	0.490
1/4" Green Prop.	280	1/4"	20.2	0.500

GRAY PROPELLANT

1/8" Plexiglas	651	5/16"	43.0	0.490
1/8" Plexiglas	534	1/16"	35.5	0.345
1/8" Plexiglas	548	3/32"	36.6	0.345
1/8" Plexiglas	473	3/32"	31.3	0.240
1/8" Aluminum	595	1/8"	46.0	0.350
0.09 Steel	508	5/16"	40.0	0.345
0.09 Steel	434	5/32"	34.5	0.490
0.99 Steel	548	1/8"	43.0	0.240
1/4" Gray Prop.	508	1/8"	38.6	0.490
1/4" Gray Prop.	501	1/8"	38.3	0.340
1/4" Gray Prop.	508	7/32"	30.6	0.340

* Critical spalling velocity

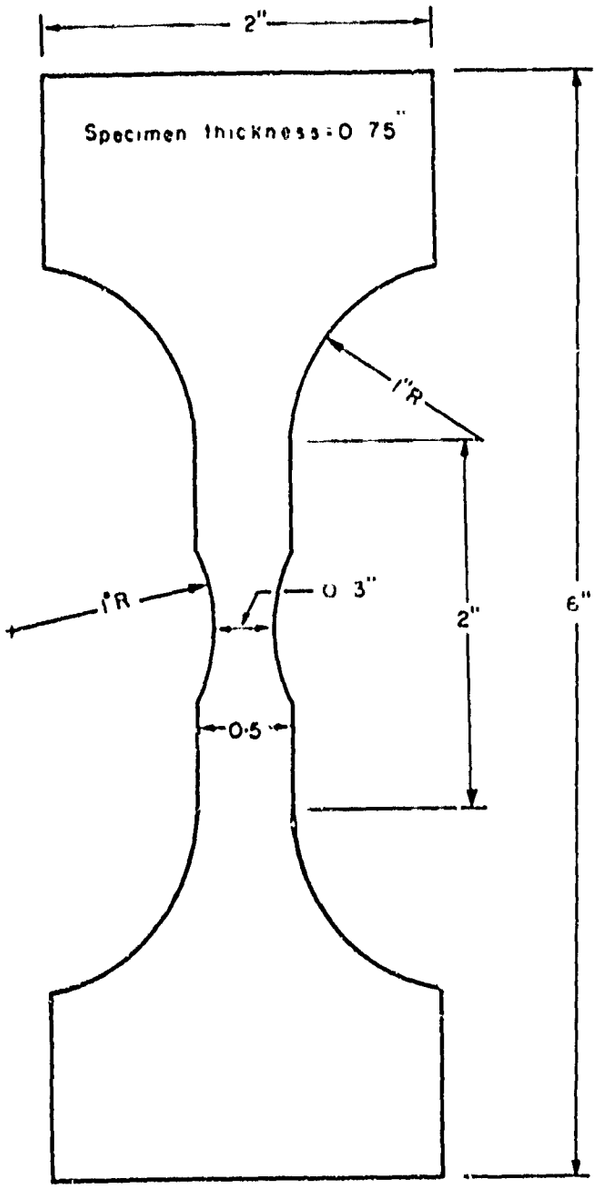

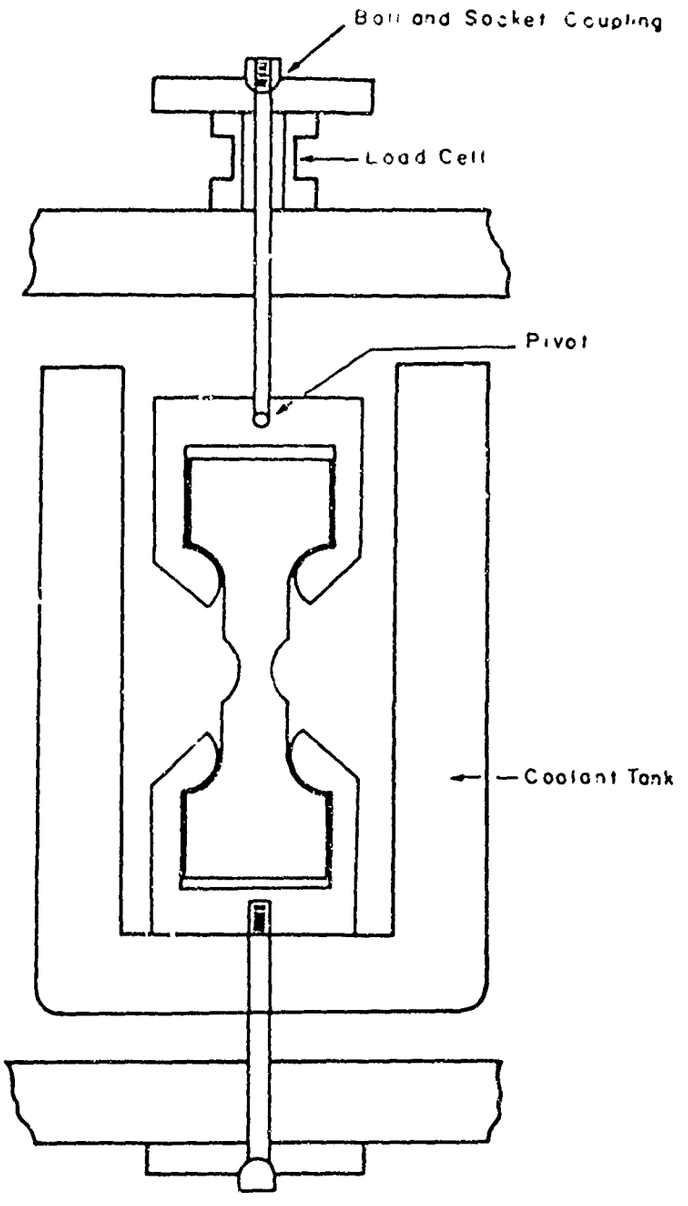

Fig. 2.1 - Tension test set up for JANAF-type specimen

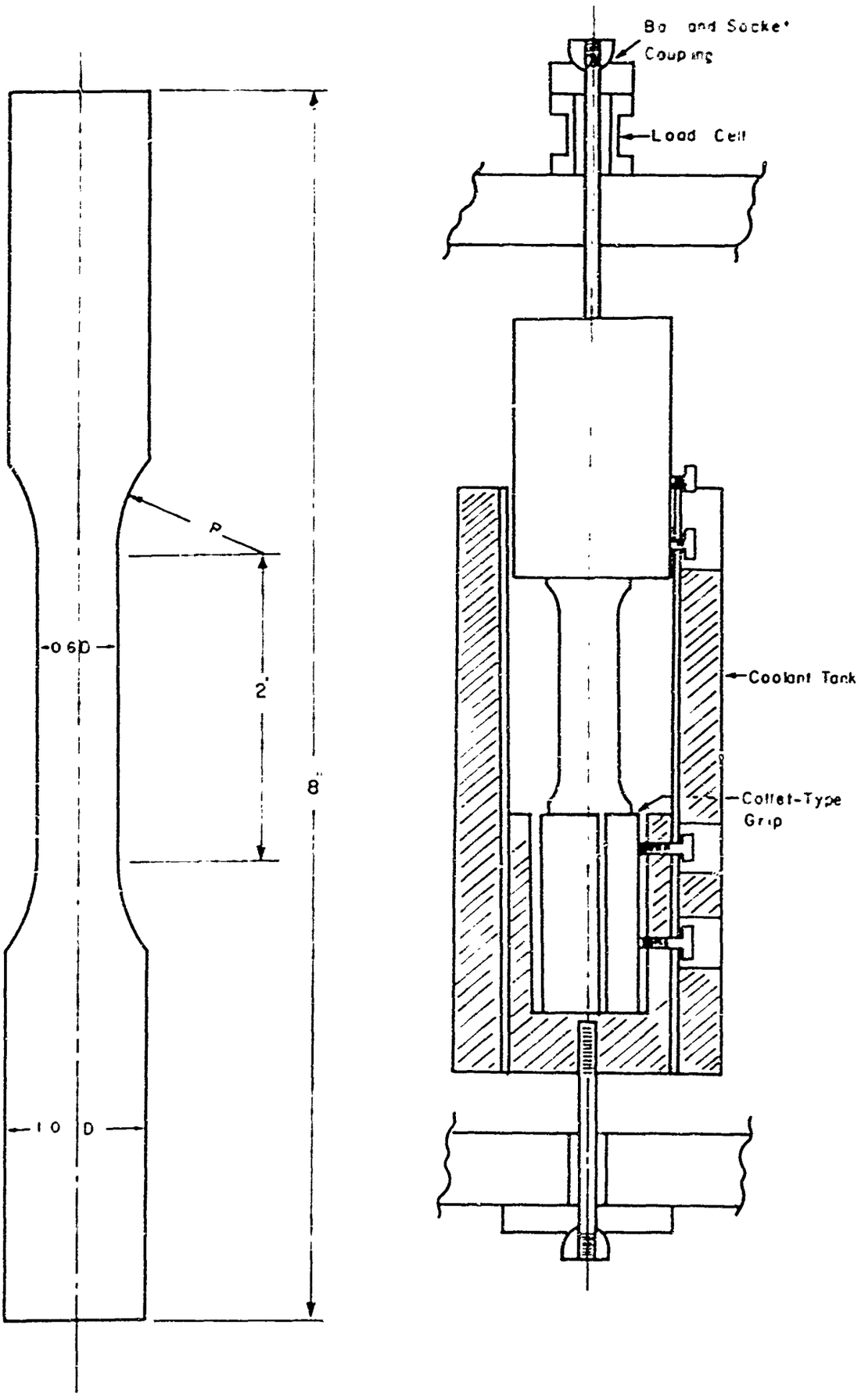

Fig. 2.2 - Tension test set up for cylindrical specimen

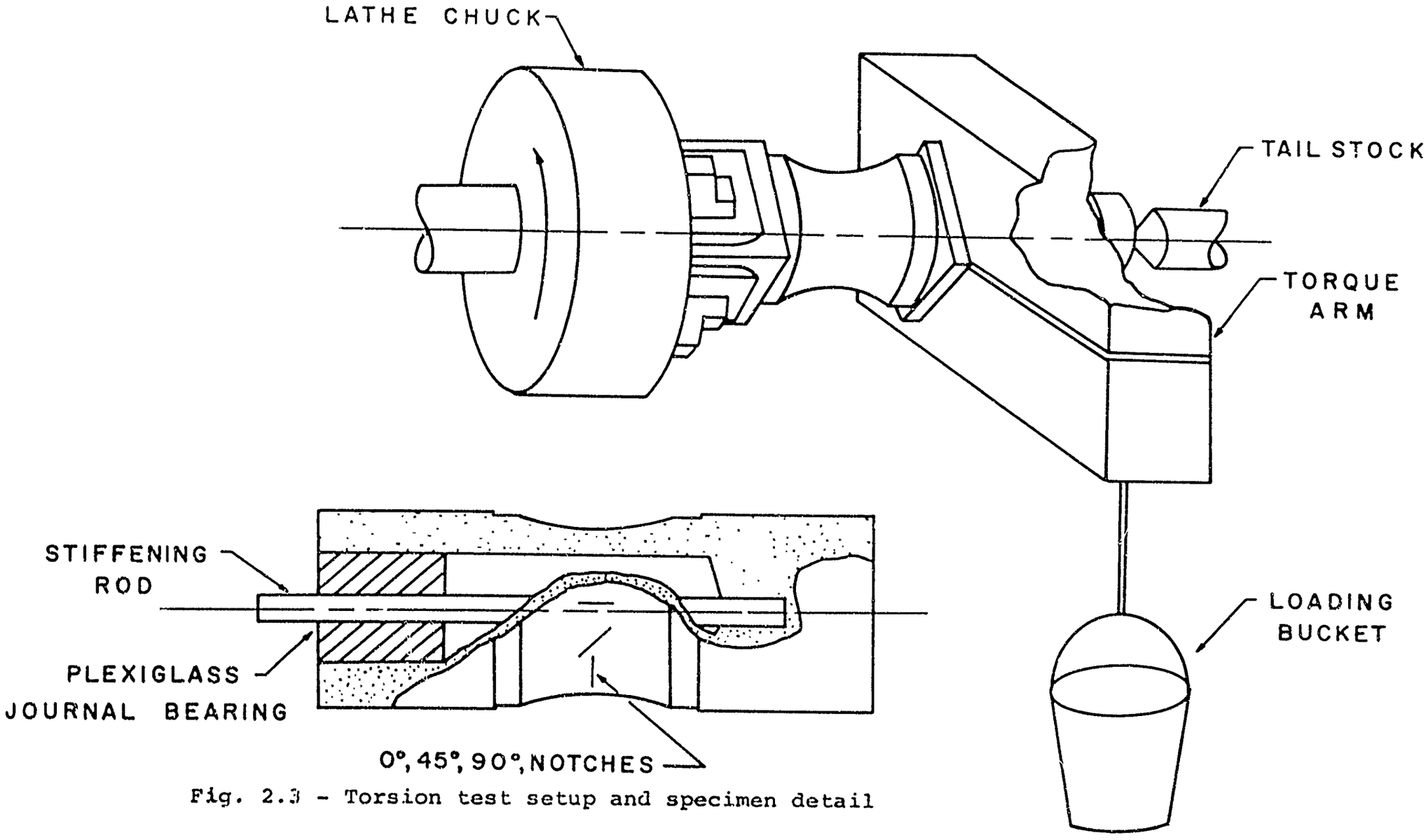

Fig. 2.3 - Torsion test setup and specimen detail

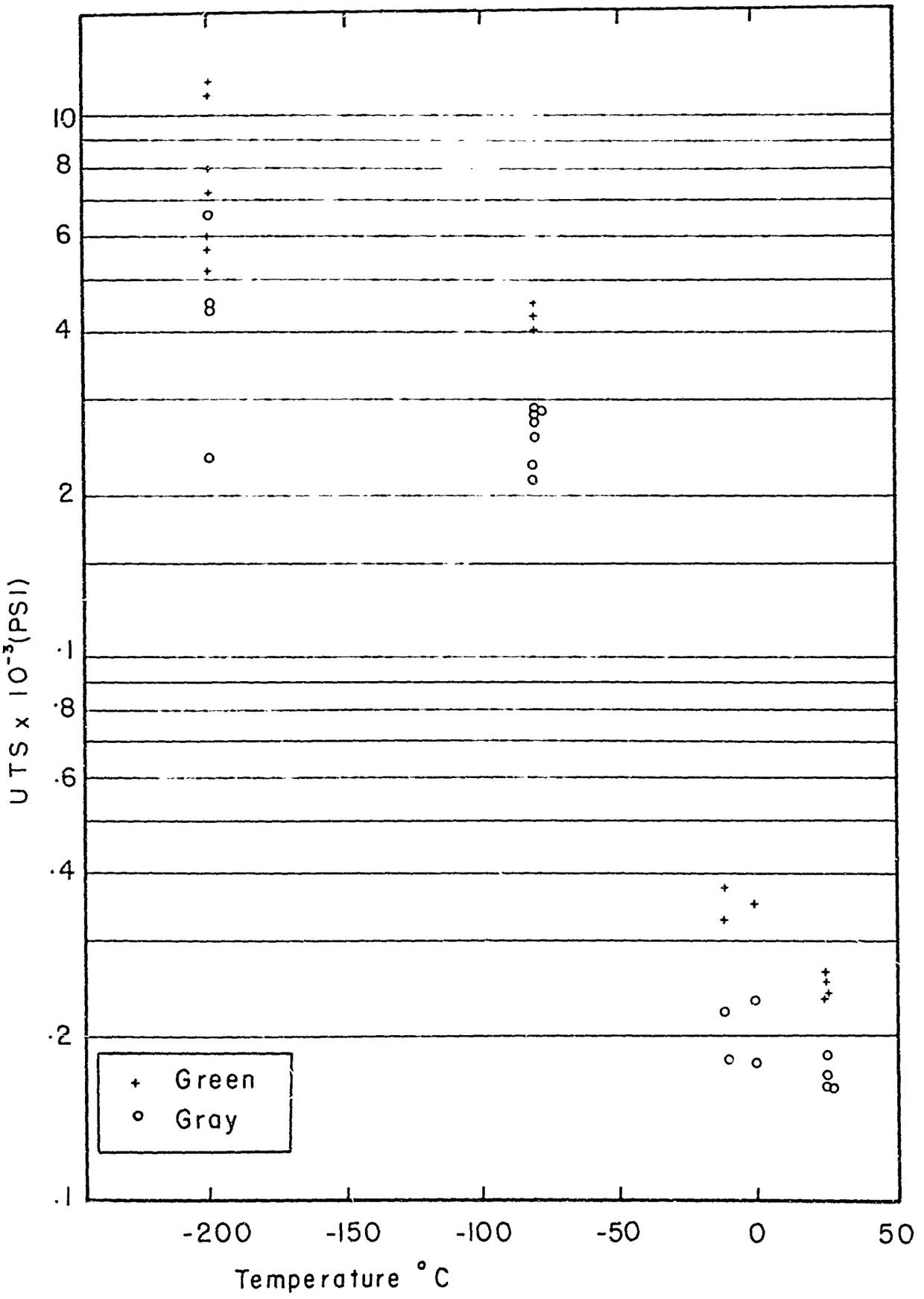

Fig. 2.4 - U.T.S. vs. temperature

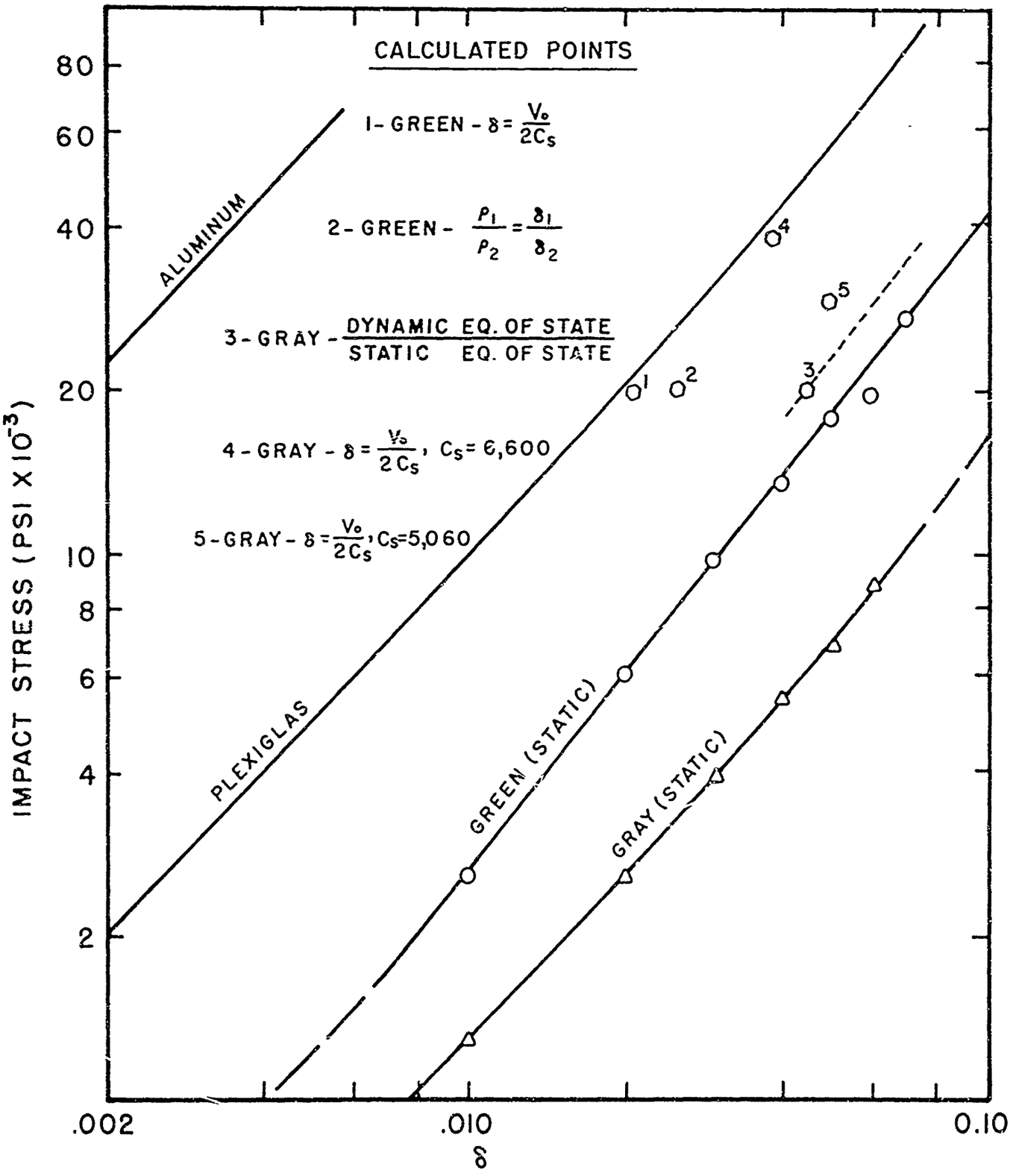

FIG. 3.1- HUGONIOT CURVES FOR TEST MATERIALS

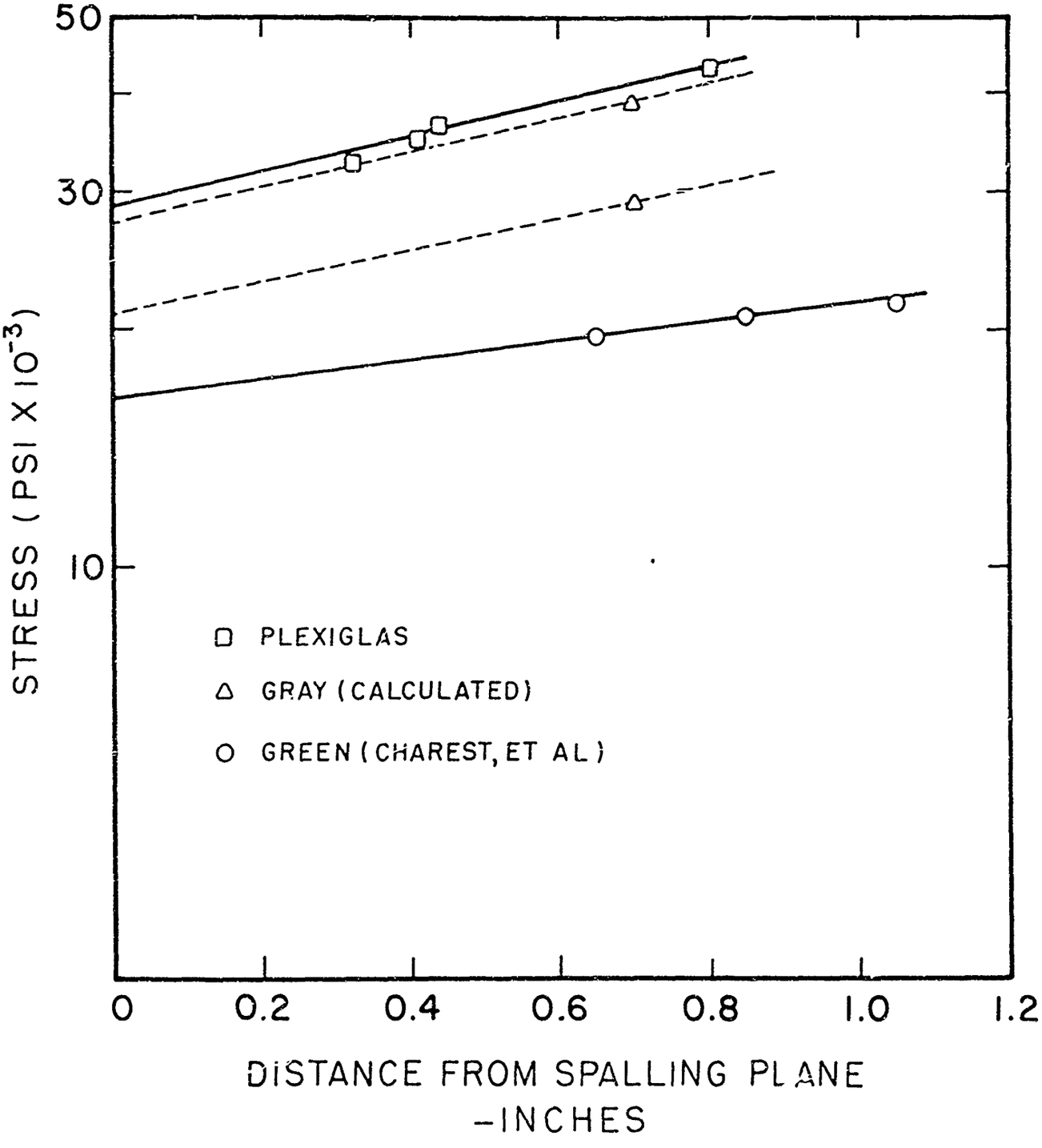
50
30
10
STRESS (PSI X 10^{-3})
PLEXIGLAS
GRAY (CALCULATED)
GREEN (CHAREST, ET AL)
0
0.2
0.4
0.6
0.8
1.0
1.2
DISTANCE FROM SPALLING PLANE
-INCHES

FIG. 3.2

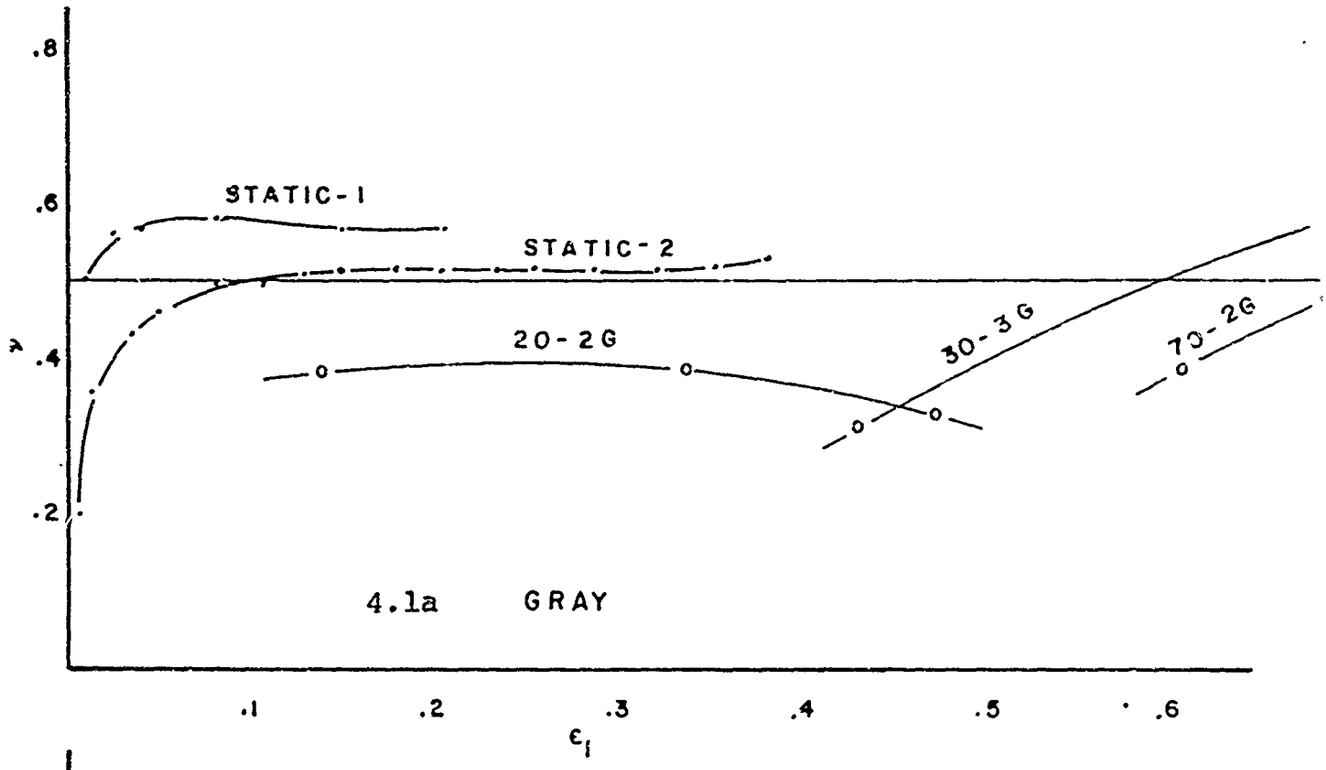

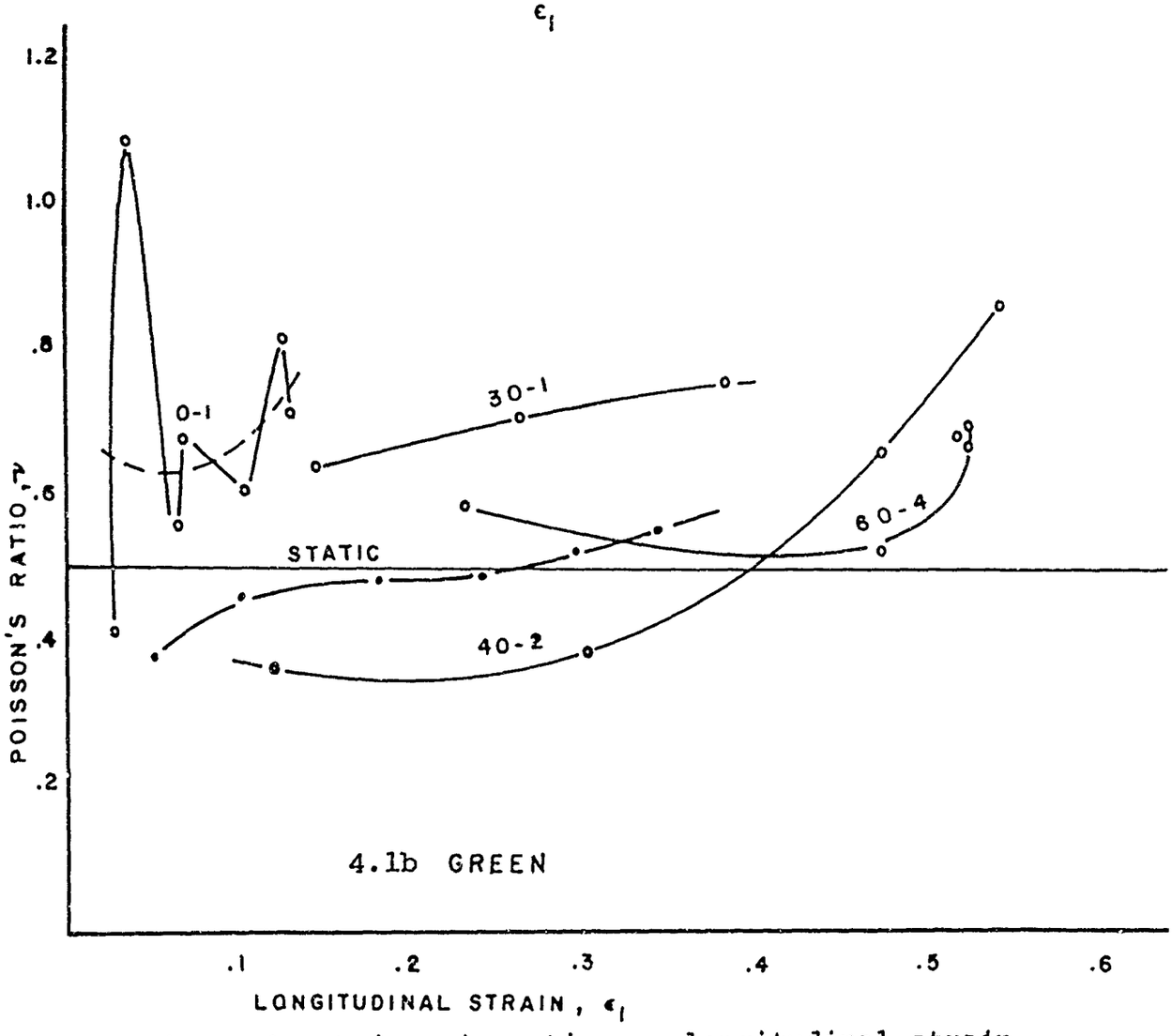

Fig. 4.1 - Poisson's ratio vs. longitudinal strain